Mould Filling Simulation in High Pressure Die Casting by Meshless Method

S. Kulasegaram*, J. Bonet, R. W. Lewis and M. Profit

School of Engineering
University of Wales Swansea, Singleton Park, Swansea SA2 8PP, U.K.
e-mail: S.Kulasegaram@swansea.ac.uk

Key words: Mould filling, High Pressure Die Casting, meshless method, SPH, CSPH

Abstract
Simulation of mould filling in high pressure die casting has been an attractive area of research for many years. Several numerical methodologies have been adopted in the past to study the flow behaviour of the molten metal inside the die cavities. However, many of these methods require stationary mesh or grid which limits their ability in simulating highly dynamic and transient flows encountered in high pressure die casting processes. In recent years, the advent of meshfree methods have led to the opening of new avenues in numerical computational field. Consequently, particle based methods have emerged as an attractive alternative for modeling mould filling simulation in pressure die casting processes. In this paper the Corrected Smooth Particle Hydrodynamics (CSPH) method is used to simulate fluid flow in the high pressure die casting cavity. CSPH is a Lagrangian method based on Smooth Particle Hydrodynamics (SPH) techniques. In CSPH method, the quantities determining the flow are localised on set of particles, which move with the flow. This enables the method to easily follow complex free surfaces, including fragmentation. This paper mainly deals with the formulation of governing equation required CSPH simulation of high pressure die casting process and presents a number of numerical results to demonstrate the capabilities of the numerical model.

1   Introduction

High pressure die casting process is widely used for mass production of components based on aluminium, magnesium or zinc alloys. In high pressure die casting, molten alloy is injected into a metal mould, called the die, and then solidification of the alloy creates the desired shape. During a high pressure die casting cycle, molten metal is initially poured into the shot sleeve and then injected into the die cavity by the plunger under pressure [1]. After die cavity is filled, pressure intensification occurs during the solidification to reduce the amount of gas porosity, feed shrinkage porosity and dimensional inaccuracies. Finally, the die is opened and casting is separated from the die. Among these steps the mould filling sequence is the crucial part to the quality of the casting. Improvements to both product quality and process productivity can be brought about through improved die design. These include developing more effective control of the die filling and die thermal performance. Numerical simulation offers a powerful and cost effective way to study the effectiveness of different die designs and filling processes. Conventional computational modelling techniques such as finite element, finite volume and volume of fluid methods have been used with reasonable success to model low pressure slow die casting processes [2,3]. However, these methods are unable to cope with the extremely complex free surface behaviour found in high pressure die casting.

The aim of this paper is to present a Lagrangian particle method for mould filling simulation in high pressure die casting process. The meshless method used in the present work is based on SPH techniques called the corrected SPH [4,5] method. This is a truly meshfree Lagrangian method. The particles are the computational framework on which governing equations are solved. The Lagrangian nature of the method makes it particulary suited for fluid flows that involve droplet formation, splashing and complex free surface motion. In the past SPH and CSPH methods have been successfully used in numerical simulations of various engineering applications [4-8]. In recent years Clearly et al [9] developed a procedure for numerical simulation of high pressure die casting based on traditional SPH techniques. Present work deviates significantly from the previous approach by formulating governing equations based on a variational framework and introducing a variationally consistent method to handle contact boundary conditions. In addition, this paper presents a number of numermical examples to demonstrate the successful implementation of the numerical procedure.

2   Numerical Methodology

The Corrected Smooth Particle Hydrodynamics (CSPH) [4,5] method is developed based on Smooth Particle Hydrodynamics(SPH) techniques [6-8]. The SPH method approximates a given function $f(x)$ and its gradient $\nabla f(x)$ in terms of values of the function at a number of neighbouring particles and kernel function $W(x - x_b, h) = W(x, h_b)$ as,

$$f_h(x) = \sum_{b=1}^{M} V_b f_b W_b(x, h_b) \quad \text{and} \quad \nabla f_h(x) = \sum_{b=1}^{M} f_b g_b(x) \tag{1}$$

where h is the smoothing length and determines the support of the kernel (see figure 1); V_b denotes a tributary volume associated to particle b generally evaluated as the particle mass divided by density; and in the traditional SPH formulations, the gradient vectors g are simply $g_b = V_b \nabla W_b$. However, in corrected SPH methods gradient functions are amended to ensure that the gradient of a general

constant or linear function is correctly evaluated. This requirement leads to two simple conditions for these gradient vectors, namely:

$$\sum_{b=1}^{M} g_b(x) = 0 \quad \text{and} \quad \sum_{b=1}^{M} x \otimes g_b(x) = I \tag{2}$$

One simple way of fulfilling the above conditions can be obtained by introducing a vector and tensor correction terms, ε and $\mathbf{L}$ respectively, to give:

$$g_b(\mathbf{x}_a) = V_b \mathbf{L}_a \left[\nabla W_b(\mathbf{x}_a) + e_a d_{ab} \right] \tag{3}$$

Substituting this equation into equation (2) leads to explicit equations for the correction terms as:

$$e_a = -\sum_{b=1}^{M_a} V_b \nabla W_b(\mathbf{x}_a) \quad \text{and} \quad \mathbf{L}_a = \left[\sum_{b=1}^{M_a} V_b (\mathbf{x}_b - \mathbf{x}_a) \otimes \nabla W_b(\mathbf{x}_a) \right]^{-1} \tag{4}$$

Evaluation of these terms will enable the second expression in equation (1) to yield the correct gradient for constant and linear functions. A detailed description of various methodologies that can be adopted to fulfill the conditions in equation (2) can be found in the literature [4,5].
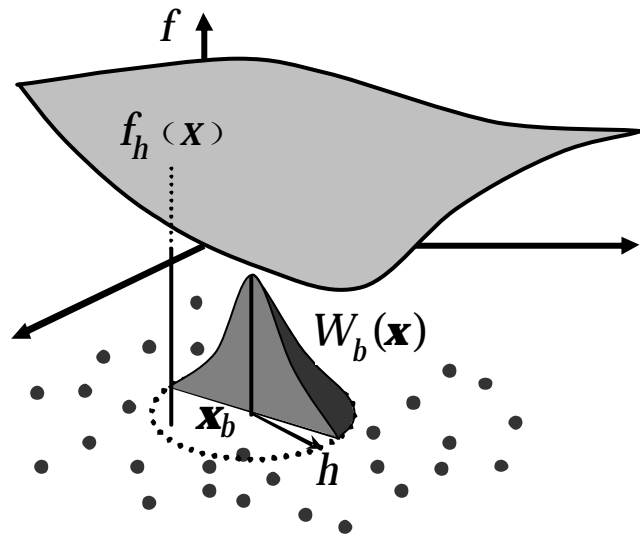

Figure 1: SPH Interpolation

3   Governing Equations

This section briefly describes the formulation of governing equations based on SPH interpolation techniques. To formulate the descrete form of the equations of motion, a Lagrangian description of a continuum is considered.   A continuum is represented by a large set of particles where each particle a is described by a mass m_a, a position vector $\mathbf{x}_a$, and a velocity vector v_a. In order to proceed with a

variational formulation of the equations of motion of the continuum, it is necessary to define the kinetic, internal and external energy of the system. For instance, the equations of motion can be expressed in variational form by defining total kinetic energy K, total internal energy Π_{int} and total external energy Π_{ext} as;

$$K = \frac{1}{2}\sum_a m_a \left(v_a \cdot v_a \right)$$
$$\Pi_{int} = \sum_a m_a p \left(r, .. \right) \tag{5}$$
$$\Pi_{ext} = -\sum_a m_a \left(\mathbf{x}_a \cdot \mathbf{g} \right)$$

where π the internal energy per unit mass, will depend on the deformation, density or other constitutive parameters. And g represents the gravitational field. The equation of motion of the system of particles representing the continuum can now be evaluated following the classical Lagrangian formalism to give:

$$\frac{d}{dt}\left(\frac{\partial L}{\partial v_a} \right) - \left(\frac{\partial L}{\partial \mathbf{x}_a} \right) = 0; \quad L\left(\mathbf{x}_a, v_a \right) = K\left(v_a \right) - \Pi_{int}\left(\mathbf{x}_a \right) - \Pi_{ext}\left(\mathbf{x}_a \right) \tag{6}$$

Substituting equations (5) into the above expressions leads to the standard Newton's second law for each particle as:

$$m_a a_a = \mathbf{F}_a - \mathbf{T}_a \tag{7}$$

where: a_a is the acceleration of the particle; the external forces $\mathbf{F}_a$, for the simple gravitational case, are:

$$\mathbf{F}_a = -\frac{\partial \Pi_{ext}}{\partial \mathbf{x}_a} = m_a \mathbf{g} \tag{8}$$

and the internal constitutive forces are defined as:

$$\mathbf{T}_a = \frac{\partial \Pi_{int}}{\partial \mathbf{x}_a} = \frac{\partial}{\partial \mathbf{x}_a}\sum_b m_b p\left(r_b, ... \right) \tag{9}$$

The evaluation of the internal forces will depend on the constitutive definition of the material. For an incompressible fluid by using the density equation given by,

$$r\left(\mathbf{x}_a \right) = \sum_{b=1}^{M_a} m_b W_a\left(\mathbf{x}_a, h_a \right) \tag{10}$$

an expression for internal forces can be obtained as:

$$\mathbf{T}_a = \sum_b m_a m_b \left(\frac{p_a}{r_a^2} + \frac{p_b}{r_b^2} \right)\nabla W\left(\mathbf{x}_a \right)_b; \quad p = r^2 \frac{dp}{dr} \tag{11}$$

where pressure p and the internal energy are related as shown in the second expression of the above equation.

In the context of the proposed variational formulation, viscosity can be introduced via a dissipative potential. This leads to a new term in the Lagrange equations as,

$$\frac{d}{dt}\left(\frac{\partial L}{\partial \boldsymbol{v}_a}\right) - \left(\frac{\partial L}{\partial \boldsymbol{x}_a}\right) = -\frac{\partial \Pi_{dis}}{\partial \boldsymbol{v}_a} \tag{12}$$

In general, the dissipative potential are expressed as the sum of viscous potentials per unit mass $\boldsymbol{y}$, which in turn are functions of rate of deformation tensor $\boldsymbol{d}$, as,

$$\Pi_{dis} = \sum_a m_a \boldsymbol{y}(\boldsymbol{d}); \quad 2\boldsymbol{d} = \nabla \boldsymbol{v} + \nabla \boldsymbol{v}^T \tag{13}$$

For instance, in the case of a Newtonian fluid, the viscous stresses are defined by:

$$\boldsymbol{s}^{vis} = 2\boldsymbol{m}\boldsymbol{d}'; \quad \boldsymbol{d}' = \boldsymbol{d} - \frac{1}{3}(tr\,\boldsymbol{d})\boldsymbol{I} \tag{14}$$

where $\boldsymbol{m}$ is the material viscosity and $\boldsymbol{d}'$ is deviatoric rate of deformation tensor. The gradient of the velocity at each cotinuum particle is obtained with the help of equation (1) as,

$$\nabla \boldsymbol{v}_a = \sum_{b=1}^{M_a} \boldsymbol{v}_b \otimes \boldsymbol{g}_b(\boldsymbol{x}_a) \tag{15}$$

After some algebraic manipulation the internal forces due to viscous effects can be evaluated as,

$$\boldsymbol{T}_a^{vis} = \frac{\partial \Pi_{dis}}{\partial \boldsymbol{v}_a} = \sum_b m_b \left(\frac{\boldsymbol{s}_b^{vis}}{\boldsymbol{r}_b}\right) \boldsymbol{g}_a(\boldsymbol{x}_b) \tag{16}$$

Thermal effects associated with the dynamics of the material can also be similarly incorporated with the above equations to simulate the mould filling in high pressure die casting process. The velocity and positions of the particles are updated by an explicit leap-frog time integration scheme defined by,

$$\boldsymbol{v}_a^{n+\frac{1}{2}} = \boldsymbol{v}_a^{n-\frac{1}{2}} + \Delta t\, \boldsymbol{a}_a^n; \quad \boldsymbol{x}_a^{n+\frac{1}{2}} = \boldsymbol{x}_a^n + \Delta t\, \boldsymbol{v}_a^{n+\frac{1}{2}} \tag{17}$$

4 Applications

In order to validate the above formulations and to demonstrate the ability of corrected SPH method a number of numerical simulations are performed to compare with corresponding experimental observations [10]. Two such comparisons are described in this section. In both cases experiments were carried out using water at room temperature. Figure 2 illustrates the die used in case 1. In this comparison, a die with a circular cross-section and a circular core was filled with water. The thickness of the die is 2mm and the gate velocity is 18 m/s. Both experimental and numerical simulation are shown in figures 4a and 4b. In case 2, a die geometry shown in figure 4 is used. In this experiment, the die thickness is again 2mm and gate velocity is 7.85 m/s. Numerical and corresponding experimental observations are shown in Figure 5a and 5b. It can be seen from the figures 4 and 5 that the method compares favourably with the experimental observations.
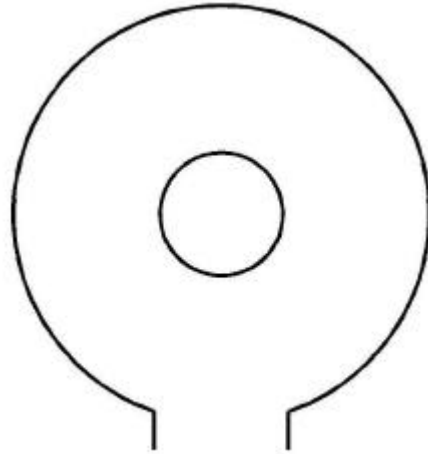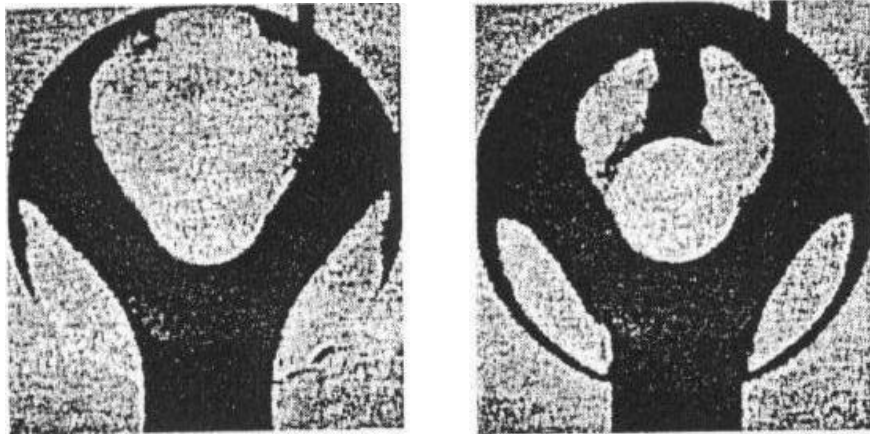
Figure 2: Die Geometry I

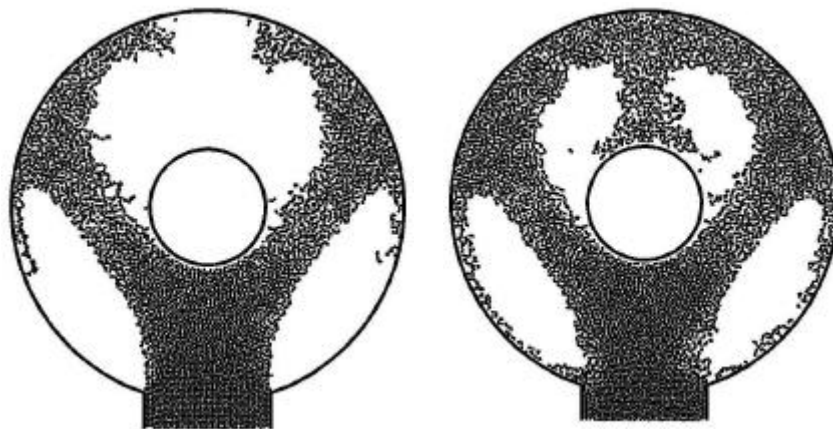
Figure 3a: Experimental results of filling die I

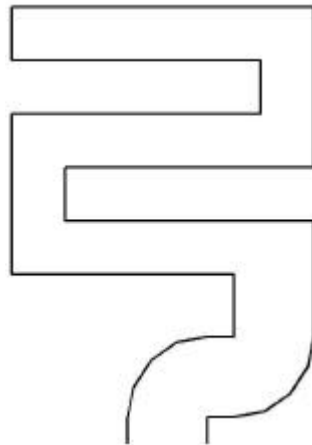Figure 3b: Numerical simulation of filling die I
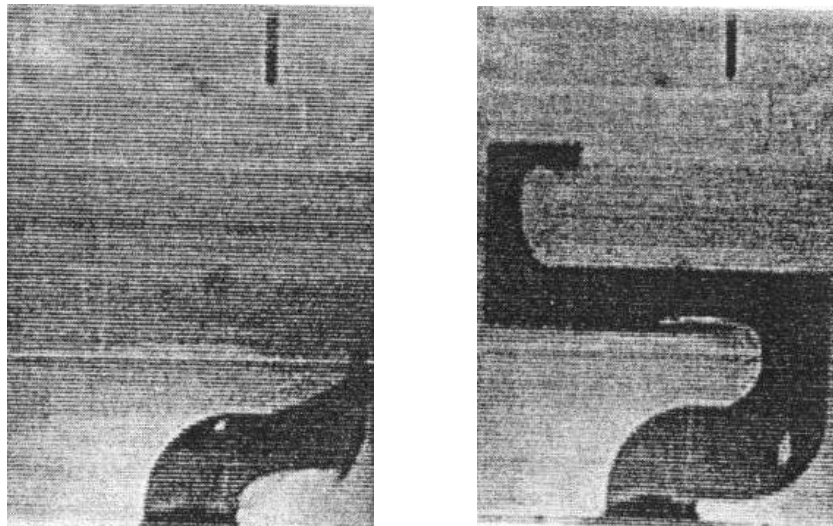
Figure 4: Die Geometry II

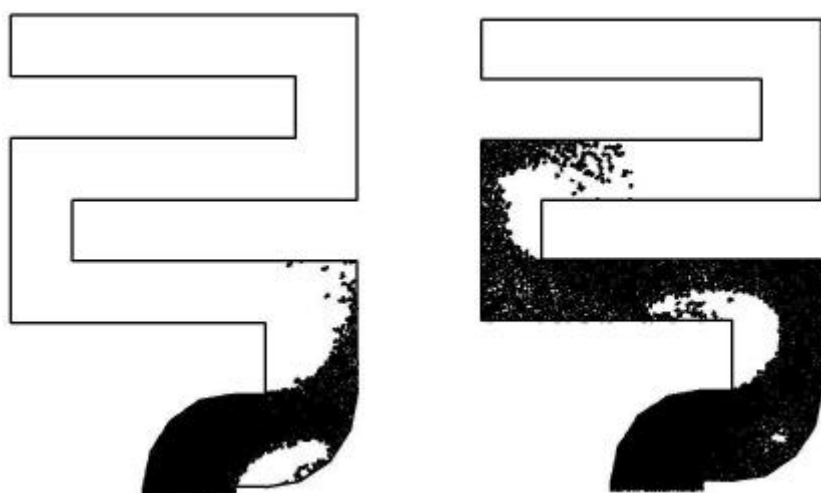Figure 5a: Experimental simulation of filling die II

Figure 5b: Numerical simulation of filling die II

References

[1] J. Barresi, Z. Chen, C. Davidson, M. T. Murray, T. Nguyen, D. H. St. John and W. R. Thorpe, *Castings of Aluminium Alloy Components,* Materials Forum (Australia), 20, (1996), 53-70.

[2] W-S. Huang and R. A. Stoehr, *Modelling Fluid Flow,* Metals Handbook Casting ASM International, 15, (1988), 867-876.

[3] R. W. Lewis and K. Ravindran, *Finite Element Simulation of Metal Casting,* Int. J. Numer. Meth. Engng., 47, (2000), 29-59.

[4] J. Bonet and T. S. Lok, *Varational and Momentum Aspects of Smooth Particle Hydrodynamics Formulations,* Comput. Methods Appl. Mech. Eng., 180, (1999), 97-115.

[5]   J. Bonet and S.Kulasegaram, *Correction and Stabilization of Smooth Particle Hydrodynamics Method with Applications in Metal Forming Simulations,* Int. J. Numer. Meth. Engng., 47, (2000), 1189-1214.

[6] L. B. Lucy, *A Numerical Approach to the Testing of Fusion Processes,* The Astronomical J., 82, 1013-1024.

[7] J. J. Monaghan, *An Introduction to SPH,* Comput. Phys. Commun., 48, (1998), 89-96.

[8] L. D. Libersky, A. G. Petschek, T. C. Carney, J. R. Hipp, F. A. Allahadi, *High Strain Lagrangian Hydrodynamics,* J. Comput. Phys., 109, (1993), 67-75.

[9] P. Cleary, J. Ha, V. Alguine and T. Nguyen, *Flow Modelling in Casting Processes,* Appl. Math. Modelling, 26, (2002), 171-190.

[10] M. Schmid and F. Klein, Fluid Flow in Die Cavities − Experimental and numerical simulation, NADCA 18. Int. Die Casting Congress and Exposition, Oct. 2-5, 1995 Indianapolis, Paper No. I-T95-034, (1995), 93-99.